Journal of Solid State Chemistry **158,** 327–333 (2001)
doi:10.1006/jssc.2001.9121, available online at http://www.idealibrary.com on IDEAL®

Syntheses and Crystal Structures of the First Bromofluorides in Niobium Cluster Chemistry: $Nb_6Br_8F_7$ and Na_2NbF_6–$(Nb_6Br_4F_{11})$

S. Cordier, O. Hernandez, and C. Perrin

Laboratoire de Chimie du Solide et Inorganique Moléculaire, UMR 6511 CNRS-Université de Rennes 1, Institut de Chimie de Rennes, Campus de Beaulieu, Avenue du Général Leclerc, 35042 Rennes Cedex, France
E-mail: stephane.cordier@univ-rennes1.fr

Received October 11, 2000; in revised form January 17, 2001; accepted February 9, 2001

We have synthesized by solid state chemistry and structurally characterized by single-crystal X-ray diffraction two new cluster compounds based on $Nb_6L^i_{12}L^a_6$ units (L = Br and/or F), namely, $Nb_6Br_8F_7$ and Na_2NbF_6–$(Nb_6Br_4F_{11})$. $Nb_6Br_8F_7$ crystallizes in the trigonal system (space group, $R\bar{3}c$; $Z = 6$; $a = 9.6373$ (6) Å; $c = 35.415$ (2) Å; $R = 0.0359$) while Na_2NbF_6–$(Nb_6Br_4F_{11})$ (space group, $Pm\bar{3}m$; $Z = 1$; $a = 8.1765$ (6) Å; $R = 0.0325$) crystallizes in the cubic system. In both structures, fluorine and bromine are randomly distributed on the inner ligand positions (L^i) that edge bridge the octahedral Nb_6 cluster. In $Nb_6Br_8F_7$, bromine fully occupies the apical ligand positions (L^a) whereas these positions are fully occupied by fluorine in Na_2NbF_6–$(Nb_6Br_4F_{11})$. The structural correlation between both compounds is discussed as well as the specificity of fluorine in the niobium cluster chemistry. © 2001 Academic Press

Key Words: **bromofluorides in niobium cluster chemistry; solid state synthesis; single-crystal X-ray diffraction; crystal structures.**

INTRODUCTION

Numerous solid state compounds containing niobium in low oxidation state are based on Nb_6L_{18} units characterized by metal–metal bonds (1). Within each unit, a Nb_6 octahedral cluster is linked to 12 edge-bridging ligands and to 6 terminal ones called inner (L^i) and apical (L^a) ligands, respectively. Such a unit is written $Nb_6L^i_{12}L^a_6$ according to the notation of Schäfer and Schnering (2). It turns out that niobium octahedral clusters are very easily obtained with chlorine, bromine, iodine, and oxygen ligands. In the latter case, the condensation of the $Nb_6O^i_{12}O^a_6$ units is very often encountered leading to band structures that can induce transport properties (4) as observed for the NbO binary compound (5). One would expect similar features in fluorides. However, this chemistry remains underdeveloped: so far, only Nb_6F_{15} has been isolated and characterized (6). On the other hand, for other niobium halides, the size of the ligands prevents strong interaction between Nb_6L_{18} units. Consequently, the molecular character of these units is preserved throughout the solid (3).

Binary cluster halides are now well known. Until recently only two M_6X_{15} structure types have been isolated: Ta_6Cl_{15} (7) and Nb_6F_{15} (6). It is noteworthy that despite great similarities between niobium and tantalum, the M_6X_{15} (X = Cl, Br, I) series has only been obtained for tantalum. For a long time Nb_6F_{15} was the only example of the Nb_6X_{15} binary halide of niobium until the synthesis of the $Nb_6Cl_{15-x}F_x$ series (8), which is isostructural to Ta_6Cl_{15}. Recently, the use of both chlorine and fluorine as ligands has led to the stabilization of pseudo-ternary Nb_6 halides that cannot be isolated by using only fluorine or chlorine (e.g., $KNb_6Cl_{10}F_5$ (10), the double salt Na_2NbF_6–$(Nb_6Cl_8F_7)$ (9), and $CsNb_6Cl_8F_7$ (10)). The structures of the two latter compounds are based on a third M_6X_{15} framework derived from Nb_6F_{15}. Fluorine has an important steric influence and leads in particular to the formation of linear bridges between units (10). The use of bromine instead of chlorine allows for a comparison of the relative influence of the fluoride and the larger halide ligands in the stabilization of Nb_6 cluster compounds.

We report in the present work the syntheses and crystal structures of the first bromofluorides, namely, $Nb_6Br_8F_7$ and Na_2NbF_6–$(Nb_6Br_4F_{11})$. The first one crystallizes in the trigonal system (space group, $R\bar{3}c$; $Z = 6$) and exhibits a novel M_6X_{15} structure type. On the other hand, Na_2NbF_6–$(Nb_6Br_4F_{11})$ crystallizes in the cubic system (space group, $Pm\bar{3}m$; $Z = 1$) with a $(Nb_6Br_4F_{11})$ network analogous to that found in Na_2NbF_6–$(Nb_6Cl_8F_7)$. It is shown that both structures can be related to each other by a simple rotation of the $(Nb_6Br^i_4F^i_8)F^{a-a}_{6/2}$ network with respect to that of $(Nb_6Br^i_5F^i_7)Br^{a-a}_{6/2}$. In both structures, the positions randomly occupied by fluorine and bromine have been discriminated allowing the determination of real Nb–F and Nb–Br bond lengths.

EXPERIMENTAL SECTION

The two bromofluorides, $Nb_6Br_8F_7$ and Na_2NbF_6–$(Nb_6Br_4F_{11})$, were prepared by solid state reactions from

0022-4596/01 $35.00

stoichiometric mixtures of NbF_5 (Aldrich, 98%), $NbBr_5$ (Ventron; purity, 99.998%), and Nb powder (Ventron, m2N8). NaBr (Merck, Pro Analysi) was added to obtain the pseudo-ternary compound. The starting powders were handled under inert atmosphere. After grinding, the sample was formed as a pellet and introduced in a niobium container (Plansee) that was then welded under argon and encapsulated in an evacuated silica tube. The final product was obtained as a black microcrystalline powder after 3 days of reaction, at a temperature ranging from 700 to 800°C. Energy dispersive spectrometry analysis performed on several selected single crystals showed that they all contained the expected elements with the same stoichiometry in each preparation.

As mentioned in the subsequent section and for clarity, the stoichiometries of the title compounds correspond to rounded values of the following refined formulas deduced from structural determinations: $Nb_6Br_{8.32(2)}F_{6.68(2)}$ and $Na_{1.9(1)}Nb_7Br_{3.6(1)}F_{17.4(1)}$, respectively.

To determine the phase breadth of $Nb_6Br_{15-x}F_x$, we performed three syntheses with three initial Br/F ratios corresponding to $Nb_6Br_{10}F_5$ (I), $Nb_6Br_{7.5}F_{7.5}$ (II), and $Nb_6Br_5F_{10}$ (III). After reaction, additional lines in the X-ray powder patterns could be attributed to Nb_3Br_8 and to a $Nb_6(Br,F)_{15}$ phase isostructural to Ta_6Cl_{15} in I and II while other unidentified phases appeared in III. The cell parameters determined by single-crystal X-ray diffraction for several crystals selected from each composition remained constant within the standard deviations. In particular, the c parameters of the single crystals used for the structural resolution were 35.415 (2) Å (I), 35.154 (1) Å (II), and 34.77 (1) Å (III), while the a parameter remains almost constant for the three compositions.

Concerning the quaternary compound, additional lines that belong to unidentified phases appear in the X-ray powder pattern when the Br/F ratio is shifted from the Na_2NbF_6–$(Nb_6Br_4F_{11})$ optimal composition. In any case, the single-crystal X-ray structural analyses lead, within the standard deviations, to the aforementioned stoichiometry of the title compound whatever the starting preparation.

STRUCTURAL DETERMINATION

The single crystals used have been synthesized according to the aforementioned procedure. The data collections have been carried out on a Nonius KappaCCD X-ray area-detector diffractometer with Mo$K\alpha$ radiation ($\lambda = 0.71073$ Å). Details about the data collections are reported in Table 1. $Nb_6Br_8F_7$ and Na_2NbF_6–$(Nb_6Br_4F_{11})$ crystallize in the trigonal and cubic systems (P network), respectively.

TABLE 1
Single-Crystal Data Collection and Structure Refinements[a]

Chemical formula	$Nb_6Br_{8.32(2)}F_{6.68(2)}$	$Na_{1.9(1)}Nb_7Br_{3.6(1)}F_{17.4(1)}$
ρ_{calc} (g cm^{-3})	4.71	3.75
Crystal dimension (mm^3)	$0.025 \times 0.046 \times 0.051$	$0.09 \times 0.116 \times 0.139$
Temperature (K)	293	293
Crystal system	Trigonal	Cubic
Space group	$R\bar{3}c$	$Pm\bar{3}m$
Lattice constants (Å)	$a = 9.6373$ (6), $c = 35.415$ (2)	$a = 8.1765$ (6)
Cell volume (Å^3)	2848.6 (3)	546.64 (7)
Z	6	1
Range of data collection (°)	$1.00 < \theta < 34.97$	$1.00 < \theta < 34.97$
μ(Mo$K\alpha$) (mm^{-1})	21.9	9.9
Absorption correction	Multiscan (13)	Multiscan (13)
Transmission factors	0.528 to 0.556	0.177 to 0.234
Total measured reflections	7728	2052
Unique reflections	1398	236
Observed reflections	803	221
R (observed reflections)	0.0359	0.0325
R_w (observed reflections)	0.0378	0.0399
S (goodness-of-fit)	1.03	1.07
unst (weighting scheme)	2	2
Variable parameters	52	31
Extinction coefficient	0.06 (1)	0.05 (2)
Max Δ/σ	0.0039	0.0021
Difference Fourier map (e Å^{-3}]	− 1.46 to 1.50	− 1.97 to 1.48

Note. $R = \sum_{hkl} \| F_o| - |F_c| \| / \sum_{hkl} |F_o|$; $R_w = \sqrt{\sum_{hkl} w'(|F_o| - |F_c|)^2 / \sum_{hkl} w' |F_o|^2}$; $w' = w/4F_o^2$; $w = 1/(\sigma^2(F_o) + (0.01 \times \text{unst} \times F_o)^2)$; $S = \sqrt{\sum_{hkl} w(F_o - F_c)^2/(m-n)}$ (n is the number of unique reflections, m the number of parameters). The refinements are done against F. Extinction correction: Becker–Coppens type 1 Lorentzian isotropic.

[a] A Nonius KappaCCD diffractometer was used for data collection (Mo tube, graphite monochromator); corrections for Lorentz and polarization effects were applied.

The structures of two $Nb_6Br_{15-x}F_x$ single crystals synthesized from the I and II starting compositions have been solved. The poor quality of crystals obtained from composition III only allowed the determination of the unit-cell parameters. We shall report in detail only the structural results obtained for composition I.

Data were processed using KappaCCD analysis software (11, 12); the cell parameters were refined to the following values: $a = 9.6373$ (6) Å and $c = 35.415$ (2) Å for $Nb_6Br_8F_7$ and $a = 8.1765$ (6) Å for Na_2NbF_6–$(Nb_6Br_4F_{11})$. A multiscan absorption correction has been carried out through SORTAV (13). Among the possible space groups deduced from the extinction conditions, the refinement procedure has unambiguously confirmed the $R\bar{3}c$ and $Pm\bar{3}m$ groups for $Nb_6Br_8F_7$ and Na_2NbF_6–$(Nb_6Br_4F_{11})$, respectively. Both structures have been solved by direct methods (program SIR97 (14)). The least-squares refinement and Fourier syntheses have been realized with the beta version of JANA2000 (15).

During the refinement it became apparent that the inner bromine sites were not fully occupied by bromine, within the estimated standard deviations. Fluorine was then introduced with the same positional and thermal parameters as bromine but the sum of their occupancies was restricted to the value corresponding to a fully occupied position. The first two restraints were then progressively relaxed resulting in the convergence of the refinement leading to final positions in agreement with reliable Nb–(Br, F) interatomic distances. Once the skeleton of Na_2NbF_6–$(Nb_6Br_4F_{11})$ was refined, the Na cation was located by Fourier difference syntheses. A Gram-Charlier expansion (16) of the anisotropic displacement parameters of the Br1 and Nb1 atoms, for $Nb_6Br_8F_7$ and Na_2NbF_6–$(Nb_6Br_4F_{11})$, respectively, was been used up to the fourth-order. In addition, the F2 atom of the former structure was refined with an isotropic thermal parameter. The final residual factors were $R = 3.59\%$ (for 803 $I > 3\sigma(I)$ observations versus 52 least-squares parameters) and $R = 3.25\%$ (for 221 $I > 2\sigma(I)$ observations versus 31 least-squares parameters) for $Nb_6Br_8F_7$ and Na_2NbF_6-$(Nb_6Br_4F_{11})$, respectively. Details on the structure refinement parameters are reported in Table 1. The final atomic parameters and selected geometrical parameters are reported in Tables 2, 3, and 4, respectively.

RESULTS AND DISCUSSION

The crystal structure of $Nb_6Br_8F_7$ is based on a $(Nb_6Br^i_5F^i_7)Br^{a-a}_{6/2}$ unit (Fig. 1) interconnected by bent Nb–Br^{a-a}–Nb bridges. The interconnection of a given unit with the six adjacent ones is represented in Fig. 2 and a projection of the unit-cell along the [010] direction is shown in Fig. 3. The apical bromine is located on an 18*e* Wyckoff special position, while all the other sites correspond to 36*f* Wyckoff general positions. Niobium and fluorine fully occupy two of these general positions, while the third one is randomly occupied by bromine and fluorine. In $Nb_6Br_{8.32}F_{6.68}$ (I), the Br/F ratio of the latter site is larger than that in $Nb_6Br_{7.99}F_{7.01}$ (II). We can thus conclude that the range of homogeneity of $Nb_6Br_{15-x}F_x$ is due to a Br/F random distribution on only 6 inner positions among the 12 possible ones, whereas in $Nb_6Cl_{15-x}F_x$, a Cl/F random distribution appears on the 12 inner as well as on the 6 apical positions. The Nb–Nb bond lengths bridged by fluorine (2.8531 (1) Å) are shorter than those randomly bridged by bromine and fluorine (2.9171 (7) Å). It is well known (3) that the HOMO level of the molecular orbital diagram calculated for the $M_6L^i_{12}L^a_6$ unit has a metal–metal bonding character but a metal–inner ligand antibonding character. Consequently, the removal of one electron from this level leads to an increase in the Nb–Nb bond lengths and to a decrease in the Nb–L^i ones. Even though the valence orbitals of the apical ligands do not contribute to the HOMO level, the Nb–L^a interatomic distance decreases in the meantime because of both electronic and steric L^i/L^a interactions. The Nb–Br^a bond length observed in the present work for $Nb_6Br_8F_7$ (2.711 (1) Å), VEC (valence electron count) of 15, is effectively shorter than that in other niobium bromides displaying a VEC of 16 like $K_4Nb_6Br_{18}$ (17) or $CsErNb_6Br_{18}$ (18) (2.812 (2) Å, 2.755 (2) Å, or 2.885 (2) Å, respectively).

TABLE 2
Fractional Atomic Coordinates and Equivalent Isotropic Displacement Parameters (Å²) for $Nb_6Br_8F_7$

Atom	Wyckoff position	Site symmetry multiplicity	Refined multiplicity	*x*	*y*	*z*	U_{equiv}
Nb	36*f*	1		0.84849 (6)	0.03379 (6)	0.03399 (1)	0.0185 (2)
Br1	18*e*	0.5		0	0.7561 (2)	$\frac{3}{4}$	0.0336 (9)
Br2	36*f*	1	0.887 (4)	0.5808 (1)	− 0.14593 (8)	0.00040 (2)	0.0272 (3)
F2	36*f*	1	0.113 (4)	0.664 (6)	− 0.129 (4)	− 0.0013 (9)	0.035 (8)
F3	36*f*	1		0.8198 (4)	− 0.1477 (4)	0.0697 (1)	0.026 (1)

Note. Refined multiplicity = occupancy × (site symmetry multiplicity); $U_{equiv} = (\frac{1}{3})\sum_i[\sum_j U_{ij}a^*_i a^*_j a_i a_j]$.
Calculated formula, $(Nb_6Br^i_{5.32(2)}F^i_{6.68(2)})Br^{a-a}_{6/2}$. Estimated standard deviations are shown in parentheses.

TABLE 3
Fractional Atomic Coordinates and Equivalent Isotropic Displacement Parameters (Å^2) for Na_2NbF_6–($Nb_6Br_4F_{11}$)

Atom	Wyckoff position	Site symmetry multiplicity	Refined multiplicity	x	y	z	U_{equiv}
Nb1	6*f*	0.125		0.7434 (2)	$\frac{1}{2}$	$\frac{1}{2}$	0.0266 (5)
Nb2	1*a*	0.02083		0	0	0	0.113 (1)
F1	12*j*	0.25	0.174 (2)	0.753 (1)	$\frac{1}{2}$	0.753 (1)	0.044 (2)
Br1	12*j*	0.25	0.076 (2)	0.8079 (4)	$\frac{1}{2}$	0.8079 (4)	0.058 (1)
F2	3*c*	0.0625		0	$\frac{1}{2}$	$\frac{1}{2}$	0.102 (4)
F3	6*e*	0.125		0	0	− 0.226 (2)	0.27 (1)
Na	12*h*	0.25	0.039 (2)	0.082 (3)	$\frac{1}{2}$	0	0.08 (1)

Note. Refined multiplicity = occupancy × (site symmetry multiplicity); $U_{equiv} = (\frac{1}{3})\sum_i[\sum_j U_{ij} a_i^* a_j^* a_i a_j]$.
Calculated formula, $Na_{1.9(1)}NbF_6$–$(Nb_6Br^i_{3.6(1)}F^i_{8.4(1)})F^{a-a}_{6/2}$. Estimated standard deviations are shown in parentheses.

However, this effect is overemphasized by the presence of fluorine on inner positions. Such a decrease in the inner bromine steric hindrance around the metallic atoms forming the cluster has been previously obtained by the replacement of bromine by oxygen ligand in $LuTa_6Br^i_9O^i_3Br^{a-a}_{4/2}Br^a_2$ (19). This similarity between fluorobromides and oxybromides is related to a similar covalent radius between oxygen and fluorine atoms (20).

The structure of Na_2NbF_6–($Nb_6Br_4F_{11}$) is built on $(Nb_6Br^i_4F^i_8)F^{a-a}_{6/2}$ units interconnected by linear Nb–F^{a-a}–Nb bridges (Fig. 4) and appears therefore to be isostructural to Na_2NbF_6–($Nb_6Cl_8F_7$). Four bromine and eight fluorine atoms are randomly distributed on the 12 12*j* inner positions of the unit, while fluorine fully occupies the 3*c* apical positions. The Nb–F^{a-a} and Nb–F^i distances are similar to those found in Na_2NbF_6–($Nb_6Cl_8F_7$). Although the covalent radius of the bromine ligand is larger than that of the chlorine one (1.82 Å versus 1.67 Å (20)), it appears that the Nb–Nb bond lengths are shorter in the bromofluoride than in the chlorofluoride (2.814 (1) Å versus 2.831 (2) Å (9), respectively). This apparent contradiction can be understood if one takes into account the fact that the average of the ligand–covalent radius weighted with respect to the Br/F or Cl/F ratio remains roughly constant for both compounds. In other words, the matrix effect due to the larger size of bromine compared to chlorine is counterbalanced by a ratio of fluorine in the bromofluoride higher than that in the chlorofluoride.

TABLE 4
Selected Geometrical Parameters (Å,°)

	$Nb_6Br_8F_7$		$Na_2Nb_7Br_4F_{17}$
Nb–Nb	2.8531 (1)	Nb1–Nb1	2.814 (1)
	2.9171 (7)	Nb1–F1	2.070 (1)
Nb–Br2	2.5698 (8)	Nb1–Br1	2.572 (3)
	2.586 (1)	Nb1–F2	2.098 (1)
Nb–F2	2.09 (3)	Nb2–F3	1.85 (2)
	1.94 (6)	Na–F1	2.42 (2)
Nb–F3	2.062 (4)	Na–Br1	2.73 (2)
	2.058 (4)	Na–F3	2.33 (2)
Nb–Br1	2.711 (1)	Nb1–F1–Nb1	85.6 (3)
Nb–Br2–Nb	68.90 (3)	Nb1–Br1–Nb1	66.3 (1)
Nb–F2–Nb	92 (2)	Nb1–F2–Nb1	180
Nb–F3–Nb	87.6 (1)		
Nb–Br1–Nb	117.23 (7)		

Note. Estimated standard deviations are shown in parentheses.

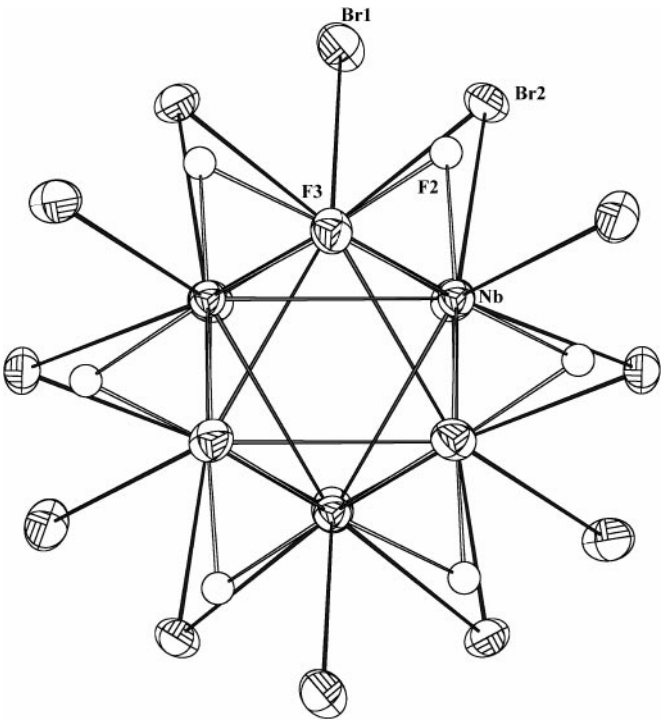

FIG. 1. $(Nb_6Br^i_5F^i_7)Br^{a-a}_{6/2}$ unit (point group $\bar{3}$) in $Nb_6Br_8F_7$. Displacement ellipsoids are shown at the 50% probability level. Only one of the two represented $Br2^i$ or $F2^i$ positions is locally occupied. Nb–Nb, Nb–F, and Nb–Br bonds are represented by grey, unfilled, and black lines, respectively.

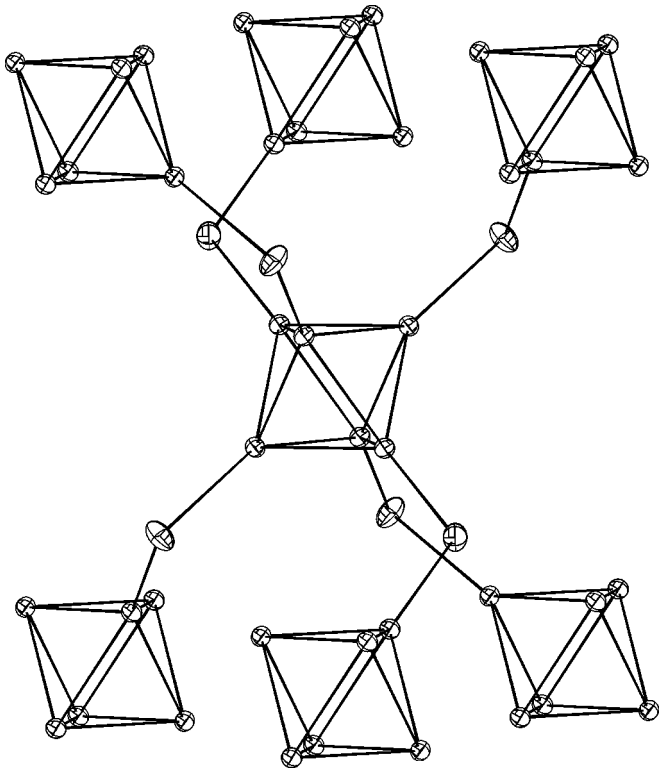

FIG. 2. Interconnection of the units in the $Nb_6Br_8F_7$ structure. For sake of clarity, the inner ligands are not represented.

The structure of Na_2NbF_6–$(Nb_6Br_4F_{11})$ consists of a $(Nb_6Br_4F_{11})$ network, sodium counter cations, and NbF_6 entities. Recall that $(MF_6)^{n-}$ entities are the basic building blocks of the $A_xM_6F_z$ complex (A, additional cation; M, transition element) that can be described as various stackings of $(MF_6)^{n-}$ octahedra sharing apices, edges or faces with neighbors. For M = Nb, the $(MF_6)^{n-}$ octahedra preferentially share their apices as encountered in Na_2NbF_7 (21) and $CoNbF_6$ (22). On the other hand, these $(NbF_6)^{n-}$ entities are found isolated in Na_2NbF_6–$(Nb_6Br_4F_{11})$ and in Na_2NbF_6–$(Nb_6Cl_8F_7)$ (9). This feature explains the high value of the anisotropic displacement parameter of the F3 atom to which the Nb2 atom is bounded. The whole Na_2NbF_6–$(Nb_6Br_4F_{11})$ structure — disregarding the Na^+ cations — derives from an ABX_3 perovskite with $A = NbF_6$, $B = (Nb_6Br_4^iF_8^i)$, and $X_3 = F_{6/2}^{a-a}$ (Fig. 5). Additional Na^+ cations are statistically distributed on a 12*h* Wyckoff position. These positions are related to each other by a fourfold axis forming a square close to the center of each face of the perovskite unit cell. The Na–F3 and the Nb–F3 interatomic distances within the NbF_6 octahedra are similar to those encountered in Na_2NbF_6–$(Nb_6Cl_8F_7)$. We can thus assume that the oxidation state of niobium in these anions for Na_2NbF_6–$(Nb_6Br_4F_{11})$ is 5 + as deduced from EPR measurements in Na_2NbF_6–$(Nb_6Cl_8F_7)$ (23). Considering an isolated Nb^{5+} cation, the number of valence electrons per cluster is calculated to be 16.

Both structures presented in this paper are based on an M_6L_{15}-type framework but differ by the kind of Nb–L^{a-a}–Nb bridges, the Br^i/F^i ratio being very close. In Ta_6Cl_{15}, one Ta_6 cluster is located at the center of a cube of Ta_6 clusters but is interconnected to only six ones by Ta–Cl^{a-a}–Ta bridges. In both present structures, one Nb_6 cluster is located at the center of an octahedron of Nb_6 clusters and is obviously bonded to all of them (for instance, see Fig. 2). It was previously found that $Nb_6Cl_{15-x}F_x$ exhibits a Ta_6Cl_{15} structure type with a random distribution of fluorine and chlorine on the inner as well as on the apical positions, whereas in Na_2NbF_6–$(Nb_6Cl_8F_7)$ fluorine is ordered only on apical positions. Hence, in the two compounds presented in this work, it turns out that the random

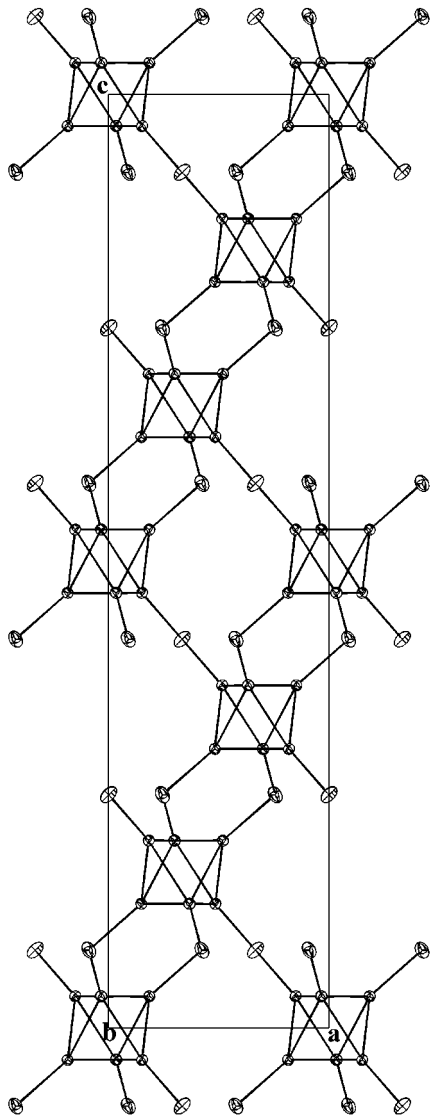

FIG. 3. Projection of the $Nb_6Br_8F_7$ structure along the [0 1 0] direction.

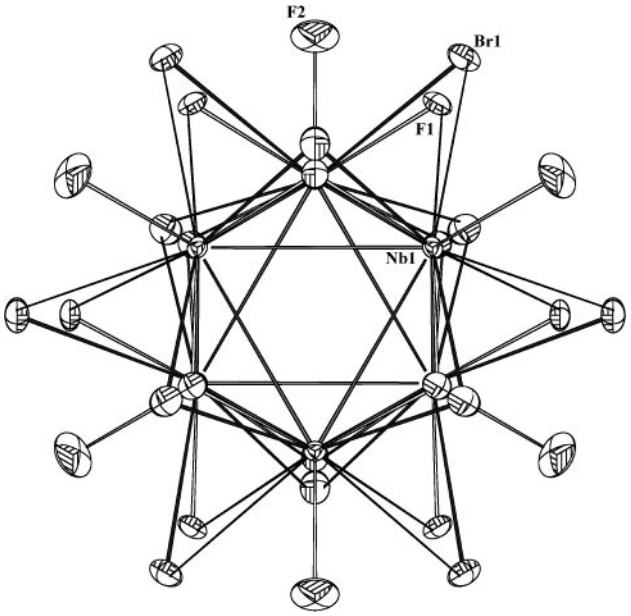

FIG. 4. $(Nb_6Br^i_8F^i_4)F^{a-a}_{6/2}$ unit (point group $m3m$) in Na_2NbF_6–$(Nb_6Br_4F_8)$. Displacement ellipsoids are shown at the 50% probability level. Only one of the two represented Br^i or F^i positions is locally occupied. Nb–Nb, Nb–F, and Nb–Br bonds are represented by grey, unfilled, and black lines, respectively.

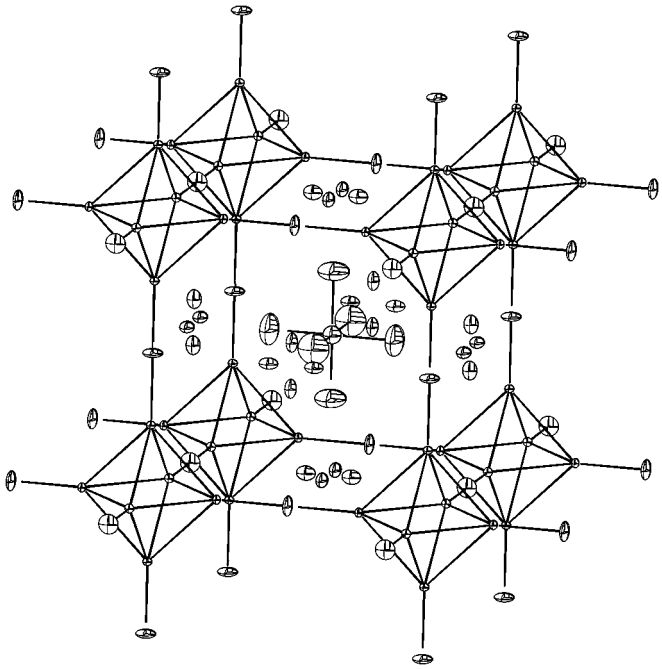

FIG. 5. Representation of the structure of Na_2NbF_6–$(Nb_6Br_4F_{11})$. For sake of clarity, the inner ligands are not represented. Displacement ellipsoids are shown at the 10% probability level.

Br/F occupation occurs on inner positions. However if such a random Br/F occupation would occur also on an apical position it would imply important structural constraint related to the large difference between the covalent radius of bromine and fluorine. In addition, the M_6X_{15} frameworks of $Nb_6Br_8F_7$ and Na_2NbF_6–$(Nb_6Br_4F_{11})$ can be related to each other even though their unit cells and formulas are very different. On one hand, the $(Nb_6Br^i_4F^i_8)F^{a-a}_{6/2}$ framework can be described by a ReO_3 structure, the $Nb–F^{a-a}–Nb$ bridges being linear. On the other hand, $(Nb_6Br^i_8F^i_7)Br^{a-a}_{6/2}$ can be described by a tilted ReO_3 structure as previously suggested for $Cs_3(ZrCl_5)Zr_6Cl_{15}Mn$ (24) and $Cs_3Zr_6Br_{15}Z$ (Z = C, B) (25). Indeed, if we compare the projection of the $(Nb_6Br^i_4F^i_8)F^{a-a}_{6/2}$ framework along [111] (Fig. 6) with the projection of a half unit-cell of $(Nb_6Br^i_5F^i_7)Br^{a-a}_{6/2}$ along [001] (Fig. 7), one can see that they are related to each other by a rotation of about 25° of the central cluster coupled to a reverse rotation of the six adjacent clusters. A hypothetical cubic $Nb_6Br_8F_7$ structure would be destabilized by the presence of a large interstitial void. In the real rhombohedral $Nb_6Br_8F_7$ structure, this void is partially filled by bromine apical ligands.

A network similar to that of $Nb_6Br_8F_7$ was previously found in zirconium chemistry (e.g., in $Cs_3(ZrCl_5)Zr_6Cl_{15}Mn$ (24) and $Cs_3Zr_6Br_{15}Z$ (Z = C, B) (25)) but several differences may be pointed out. Firstly, countercations as well as an interstitial atom within the cluster are essential to stabilize the zirconium compounds. Zirconium being less rich in electrons than niobium, additional electrons are thus added to the cluster via an interstitial element. Moreover, the latter element strengthens the cohesion of the Zr_6 cluster by Zr–Z–Zr bonds and stabilizes the HOMO level of the unit (26). However, like for niobium cluster chemistry,

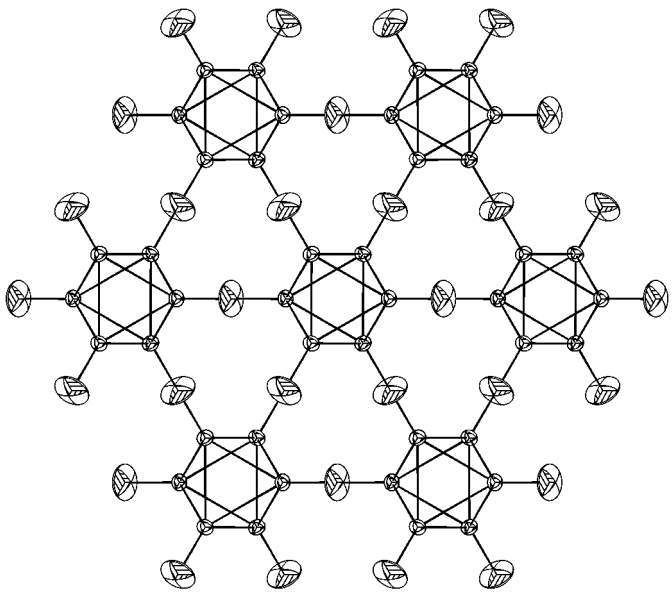

FIG. 6. Projection along the [1 1 1] direction of the $(Nb_6Br^i_4F^i_8)F^{a-a}_{6/2}$ network in Na_2NbF_6–$(Nb_6Br_4F_{11})$. For sake of clarity, the inner ligands are not represented.

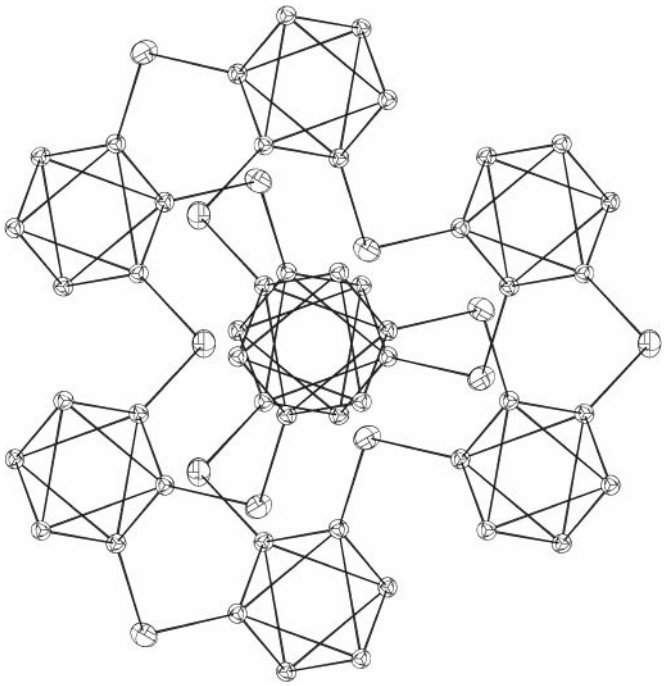

FIG. 7. Projection along the [0 0 1] direction of the $(Nb_6Br^i_5F^i_7)Br^{a-a}_{6/2}$ network in $Nb_6Br_8F_7$ (only half of the unit cell along c is shown). For sake of clarity, the inner ligands are not represented.

supplementary countercations may also bring electrons allowing in the meantime the cohesion of the structure via Coulombic interactions. Clusters in $Cs_3Zr_6Br_{15}C$ and $Cs_{3.4}Zr_6Br_{15}B$ contain, respectively, 16 and 15.4 electrons per cluster against a VEC value strictly equal to 15 for $Nb_6Br_8F_7$. The shorter Nb–Nb and Nb–Br^a bond lengths compared to the Zr–Zr and Zr–Br^a ones induce a more compact M_6X_{15} framework that does not need to be stabilized by countercations. Furthermore, in $Nb_6Br_8F_7$, the value of the Nb–Br^{a-a}–Nb angle (117.25° (7)) is lower than the corresponding one in $Cs_3Zr_6Br_{15}Z$ (134°). It is noteworthy that $Nb_6Br_8F_7$, $Cs_3Zr_6Br_{15}C$, and $Cs_{3.4}Zr_6Br_{15}B$ exhibit a close c parameter ($c = 35.415\,(2)$ Å for I; $c = 35.746\,(5)$ Å and $35.980\,(6)$ Å for $Cs_3Zr_6Br_{15}C$ and $Cs_{3.4}Zr_6Br_{15}B$, respectively). As a consequence, the structural differences between the niobium and zirconium compounds (i.e., shorter M–M and M–X^a bond lengths, absence of countercation, smaller M–X^{a-a}–M angles) lead to a contraction of the M_6X_{15} framework along the a direction ($a = 9.6373$ (6) for I; $a = 13.088\,(1)$ Å and $13.116\,(1)$ Å for $Cs_3Zr_6Br_{15}C$ and $Cs_{3.4}Zr_6Br_{15}B$, respectively).

The present study on bromofluoride cluster compounds completes the previous results on chlorofluorides (10). It turns out that the use of fluorine combined with Cl or Br ligands allows stabilization of new structure types that cannot be isolated by using only fluorine, chlorine, or bromine ligands. In particular, no binary niobium cluster chloride or bromide had been isolated with a VEC of 15. The new $Nb_6Br_8F_7$ compound is the second example, after $Nb_6Cl_{15-x}F_x$ (8), of a pseudo-binary fluorohalide displaying such a VEC. Unfortunately, we have not succeeded up to now to avoid the presence of magnetic Nb_3Br_8 impurities in the final product, preventing us from performing magnetic measurements. Last, it turns out that the replacement of chlorine by bromine leads to a decrease in the L/F ratio (L = Cl or Br), as illustrated by the examples of Na_2NbF_6–($Nb_6Cl_8F_7$) and Na_2NbF_6–($Nb_6Br_4F_{11}$).

ACKNOWLEDGMENTS

We thank the "Centre de Diffractométrie de l'Université de Rennes 1" for the data collection on the Nonius KappaCCD X-ray diffractometer. In particular, the useful advice of Dr. T. Roisnel is gratefully acknowledged. We are also very much indebted to C. Derouet for his technical help during the synthesis of the samples and to "Fondation Langlois" for its financial support.

REFERENCES

1. C. Perrin, S. Cordier, S. Ihmaïne, and M. Sergent, *J. Alloys Compd.* **229,** 123 (1995).
2. H. Schäfer and H.-G. Schnering, *Angew. Chem.* **76,** 833 (1964).
3. F. Ogliaro, S. Cordier, J.-F. Halet, C. Perrin, J.-Y. Saillard, and M. Sergent, *Inorg. Chem.* **37,** 6199 (1998).
4. G. V. Vajenine and A. Simon, *Inorg. Chem.* **38,** 3463 (1999).
5. A. L. Bowman, T. C. Wallace, J. L. Yarnell, and R. G. Wenzel, *Acta Crystallogr.* **21,** 843 (1966).
6. H. Schäfer, H.-G. Schnering, K. J. Niehus, and H. G. Nieder-Vahrenholz, *J. Less-Common Met.* **9,** 95 (1965).
7. D. Bauer and H.-G. v. Schnering, *Z. Anorg. Allg. Chem.* **361,** 259 (1968).
8. L. Le Polles, S. Cordier, C. Perrin, and M. Sergent, *C. R. Acad. Sci. Paris*, Ser. II c **2,** 661 (1999).
9. S. Cordier and A. Simon, *Solid State Sci.* **1**(4), 199 (1999).
10. S. Cordier, O. Hernandez, and C. Perrin, *J. Fluorine Chem.* **107,** 205 (2001).
11. Nonius (1999). COLLECT, DENZO, SCALEPACK, SORTAV: KappaCDD Program Package. Nonius BV, Delft, The Netherlands.
12. Z. Otwinowski and W. Minor (1997). *Methods Enzymol.* **276,** 307–326.
13. R. H. Blessing, *Acta Crystallogr. A* **51,** 33 (1995).
14. G. Cascarano, A. Altomare, C. Giacovazzo, A. Guagliardi, A. G. G. Moliterni, D. Siliqi, M. C. Burla, G. Polidori, and M. Camalli, *Acta Crystallogr. A* **52,** C-79 (1996).
15. V. Petříček and M. Dušek (2000). JANA2000: Crystallographic Computing System. Institute of Physics, ASCR, Praha, Czech Republic.
16. K. N. Trueblood, H.-B. Bürgi, H. Burzlaff, J. D. Dunitz, C. M. Gramaccioli, H. H. Schulz, U. Shmueli, and S. C. Abrahams, *Acta Crystallogr. A* **52,** 770 (1996).
17. F. Ueno and A. Simon, *Acta. Crystallogr. C* **41,** 308 (1985).
18. S. Cordier, C. Perrin, and M. Sergent, *Z. Anorg. Allg. Chem.* **619,** 621 (1993).
19. S. Cordier, C. Perrin, and M. Sergent, *Croat. Chem. Acta* **68,** 781 (1995).
20. R. P. Shannon, *Acta Crystallogr. A* **32,** 751 (1976).
21. M. B. Bournonville, D. Bizot, J. Chassaing, and M. Carton, *J. Solid State Chem.* **62,** 212 (1986).
22. J. Chassaing, C. Monteil, and D. Bizot, *J. Solid State Chem.* **43,** 327 (1982).
23. S. Cordier, C. Perrin, and J.-Y. Thépot, *unpublished* (2000).
24. J. Zhang and J. D. Corbett, *Inorg. Chem.* **34,** 1652 (1995).
25. R.-Y. Qi and J. D. Corbett, *Inorg. Chem.* **34,** 1657 (1995).
26. R. P. Ziebarth and J. D. Corbett, *J. Am. Chem. Soc.* **111,** 3272 (1989).